EXCESS HEAT REPRODUCIBILITY AND EVIDENCE OF ANOMALOUS ELEMENTS AFTER ELECTROLYSIS IN Pd|D_2O+H_2SO_4 ELECTROLYTIC CELLS

W.-S. Zhang [1,2] and J. Dash [1]

[1]Low Energy Nuclear Laboratory (LENL), Portland State University

Portland, OR 97207-0751, U.S.A., dashj@pdx.edu

[2]Institute of Chemistry, Chinese Academy of Sciences

P.O. Box 2709, Beijing 100080, China

Abstract

Electrolyte temperature is a key factor in excess heat production using Pd|D_2O+H_2SO_4 electrolytic cells. Best results are obtained when the electrolyte temperature is close to the boiling point. Stable excess heat is generated by events on or near the Pd cathode surface. In addition to the stable excess heat, heat bursts are sometimes observed. These occurred most frequently in experiments using 2 mm diameter tubes for the cathodes. Excess heat measured by isoperibolic calorimetry is directly verified by Seebeck envelope calorimetry. Experiments with D_2SO_4 replacing H_2SO_4 in heavy water electrolyte showed that there was no affect on excess heat production. After electrolysis, localized concentrations of silver were found on Pd cathode surfaces. Three characteristic surface features, (1) craters with rims containing electroplated Pt; (2) cracks in the sample; and (3) palladium regions around the cathode edges are preferred locations for the occurrence of silver.

I. Introduction

Anomalous excess thermal power in Pd|D_2O+H_2SO_4 electrolytic cells has been observed by isoperibolic calorimetry [1–3]. From 2004 to 2005, the excess power was verified by Seebeck Envelope Calorimetry (SEC) [4]. Then, no excess heat was observed in SEC experiments during an eight-month period. Eventually, we found that there is a key parameter for excess heat reproducibility in isoperibolic calorimetry which had not been satisfied in SEC. From then on, we were able to obtain excess heat output from 12 consecutive samples using

SEC. We will discuss this and other related issues in detail below.

Another previous discovery of our group is the presence of silver on the palladium surface after electrolysis in heavy water [1–6]. In this paper we will present overwhelming evidence of silver production on samples. This evidence was obtained by intensive microanalysis studies.

The experimental set-up of the electrolytic cell, power and temperature measurements, and microanalysis have been reported before [4]. We will not discuss them here, except for some recent modifications.

II. Calorimetric results

During SEC experiments, we measured three characteristic temperatures, i.e. $T_{\text{electrolyte}}$, T_{catalyst} and T_{top}, where $T_{\text{electrolyte}}$ is the temperature of electrolyte, which is measured by two K-type thermocouples attached to the bottom of the cell; T_{catalyst} is the temperature of catalyst, which is measured by three K-type thermocouples attached on the outside of the cell at the level of the catalyst; T_{top} is the temperature on the outside of the cell top, which is measured by one K-type thermocouple attached at the center of cell cap. Another point is that all excess power results reported here do not include mass loss corrections, as before [4]. This will result in null excess power for some experiments due to the loss of the heat of recombination of H_2O and D_2O resulting from the escape of H_2, D_2, and O_2 gases.

Firstly, we demonstrate the effects of the temperature difference between the SEC wall and the electrolyte, from the initial value to the steady state value of electrolyte, on excess heat production. One example is shown in Figure 1. The cell of Exp. No. 050925 was placed in a large glass beaker ($\phi 7.2 \times 11$ cm^2) to prevent leakage of electrolyte; the cell of Exp. No. 051205 was placed into a cardboard box to decrease the rate of heat flow from the cell, thus raising the cell temperature. The cardboard box size is $11.5 \times 11.5 \times 17$ cm^3, with wall thickness of 3 mm. It has a Styrofoam insert 5 cm thick with one hole ($\phi 5.7 \times 4.1$ cm^2) in its center to accommodate the electrolysis cell. We found that, along with the greatly increased temperature gradient in the latter experiment, excess heat was produced. There was no excess heat in experiment 050925, which ran at a lower temperature, with a much lower temperature gradient.

In Exp. No. 051205 and other similar experiments, a cardboard box was always used to increase the electrolyte temperature. In order to exclude the possibility that the signal of

excess power is only the effect of the heat insulation layer around the cell, we calibrated the SEC using the cardboard box with the calibration resistor inside, as in the electrolysis experiments. A resulting calibration constant is 177.04 ± 0.09 W/V, which is within the average value 176.85 ± 0.25 W/V obtained without cardboard box around that time, as shown in Table. I. This shows that excess power is not caused by the system configuration. We repeated this calibration method several times. The device constants obtained were all consistent with that obtained without the cardboard box. Because the cardboard box increases the calibration time, we rarely calibrate the SEC using this method.

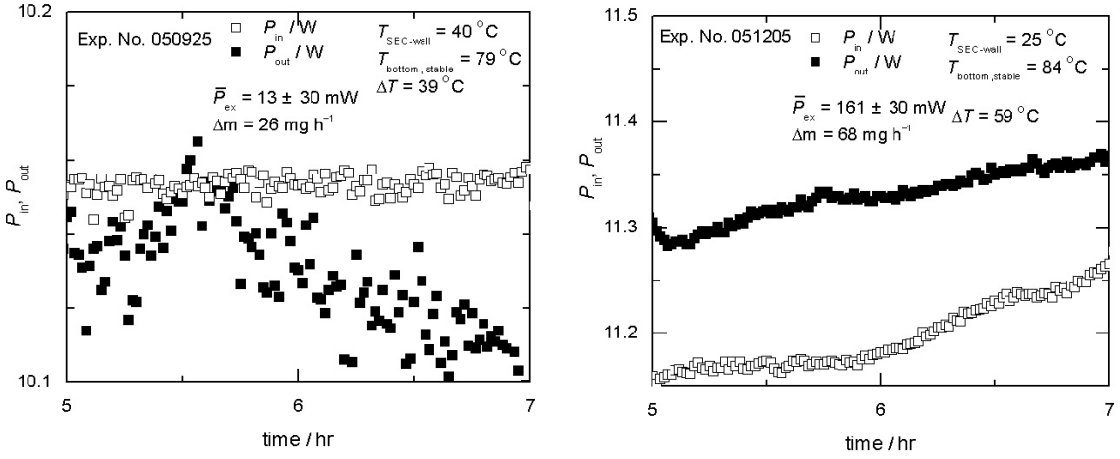

Fig. 1. An example of the effect of electrolyte temperature increment on excess heat production. The cathode in both experiments is sample Pd-E, whose parameters are shown in Table III. The applied current is 3 A, and the current density is 0.24 A cm^{-2}.

Table I. Device constants of SEC at wall temperature 25 °C during 2006

Date	Input power / W	Device constant / W V^{-1}
Apr 5	9.335 ± 0.005	176.64 ± 0.14
Apr 7*	11.073 ± 0.003	177.04 ± 0.09
May 17	11.118 ± 0.003	176.63 ± 0.13
June 4	11.103 ± 0.002	177.09 ± 0.11

* For this calibration, the resistor was in the cardboard box. For the other three calibrations, the resistor without cardboard box was used.

Another series of excess power data on background and foreground temperatures for

sample Pd-A besides that reported before [4] is shown in Table II, there is also an optimal background temperature for excess heat production as reported before [4]. All of these results indicate that both the temperature under steady-state in electrolysis and the background (or initial) temperature have important effects on excess heat. These two factors have different tendency on excess heat. High working temperature and low background temperature are important conditions for excess heat production. The cell with sample Pd-A was put in a large glass beaker only to prevent leakage of electrolyte onto the floor of the SEC; however, the low concentration of H_2SO_4 (5wt.% is one-fourth that the used ordinarily) in Table I of Ref. [4] and high current in Table II here ensure the high temperature of electrolyte, and hence excess power was observed. This suggests that every method which increases electrolyte temperature will be favorable for excess heat production. But this does not mean that lowering the SEC wall temperature and installing good heat insulation around the cell will increase excess power. We have conducted experiments at T_{wall} = 15 °C and let the steady-state electrolyte temperature be close to that at T_{wall} = 25 °C, by packing more Styrofoam around the cell with sample Pd-H; however, excess power did not change significantly. There are other unknown parameters controlling the excess power.

Table II. Excess power dependence on the initial and steady-state values of electrolyte temperatures.

Exp. No.	$T_{SEC\text{-}wall}$ / °C	$T_{electrolyte}$ / °C	ΔT / °C	P_{ex}/mW	Δm/ mg h^{-1}
050105	20	79	59	271 ± 16	11
050108	25	81	56	238 ± 15	11
050110	35	88	53	492 ± 15	64
050111	40	90	50	349 ± 15	80

Note: The cathode is sample Pd-A, its size is 0.4 × 25 × 25 mm^3, surface area is 7.1 cm^2 and its weight is 1.34 g. The applied current is 3.6 A, and the current density is 0.5 A cm^{-2}.

After finding this key factor of excess heat production, we tested previously electrolyzed samples Pd-B to Pd-D, from which it had previously been difficult to produce excess heat [4]. We found that this method was successful, as expected, as shown in Table III.

Table III. Summary of excess power for various samples from Sep 2005 to Oct 2006.

Pd No.	size/mm^3	*mass*/g	*Area*/cm^2	Exp. No.	$P_{ex,max}$/mW*	Δm/mg h^{-1}	$P_{ex,burst,\ max}$/mW**	C_{Ti}/g l^{-1}
B	0.25 × 10 × 61	2.0390	14.6	060803	178 ± 14	73	Null	0
C	0.4 × 25 × 25	3.4687	12.5	060112-060211	147 ± 37	83	197	0
D	0.05 × 11 × 31	0.1628	7.1	051221-060104	151 ± 17	31	null	0
E	0.25 × 25 × 25	1.8982	12.5	050925-060711	759 ± 33***	228	623	33
F1	0.3 × 9.4 × 24.5	0.7764	4.7	051006-051109	461 ± 20	200	null	27
F2	0.3 × 9.4 × 23	0.7346	4.4					
G	0.35 × 9 × 41	1.3875	7.6	060215-060223	97 ± 12	99	null	23
H	See Table IV			060309-060602	129 ± 14	47	355	8
I	ϕ0.67×ϕ1.67×80	1.3064	1.6	060613-060701	356 ± 11	160	1130	0
J	0.23 × 7.7 × 25	0.6080	4.9	060817	149 ± 17	191	543	0
K	0.23 × 11 × 23	1.3875	7.6	060821	339 ± 15	276	851	0
L	0.25 × 10 × 27	0.6703	5.4	060823	174 ± 12	433	null	0
M	0.27 × 11 × 26	0.7918	5.7	060825-061010	306 ± 49	506	1144	0

* $P_{ex,max}$ is the maximum stable (usually > 1 hour) excess power during electrolyses for the sample.

** $P_{ex,burst,max}$ is the maximum burst of excess power for the sample.

*** The excess heat measured by SEC is 20.54 ± 0.90 kJ at this time.

Table IV. Summary of excess power obtained for sample Pd-H with varying thickness. The current density was about 0.6 A cm^{-2} for every experiment. As received thickness was 0.5 mm. Thickness was reduced by cold rolling.

Sample size/ mm^3	Exp. No.	P_{ex}/mW	Δm/ mg h^{-1}
0.34×8.2×31	060315	68 ± 16	39
0.20×16×16	060406	129 ± 14	47
0.15×16×16	060418	107 ± 15	40
0.10×15×17	060420	65 ± 39	39
0.03×16×16	060601	122 ± 9	108

From September 2005 to October 2006, we have conducted electrochemical calorimetric measurements of Pd|D_2O+H_2SO_4 with 12 Pd samples and these samples all gave excess heat using the method described above; the results are summarized in Table III.

In these samples, Pd-F consists of two pieces which are almost the same size; these were placed in two cells connected in series. Sample Pd-H was cold rolled after each run of electrolysis; the thickness changed from the original value, 0.5 mm to 0.03 mm as illustrated in Table IV. It was found that excess power does not depend strongly on the sample thickness. This may mean that excess heat is a surface effect rather than a volume effect as suggested previously [7].

Sample Pd-I is a palladium tube. About 30 mm on one end was exposed to electrolyte during electrolysis while the upper part was covered with PTFE heat-shrinkable tubing. The anode is a concentric cylinder made of Pt foil with total area of 48 cm^2. This cathode gave maximum stable excess power of 356 ± 11 mW at input power of 9.863 W during electrolysis for 7 hours and 10 minutes in Exp. No. 060620. After electrolysis for 56 hours in this run, the cell began producing heat bursts as shown in Fig. 2. The maximum heat burst is 1.1 W. The full-width at half-maximum of the heat bursts ranges from 12 minutes at its first occurrence at about 56 hours to 3.3 minutes at 110 hrs; the period of the heat bursts ranges from 3.3 hours to a few minutes. Besides Pd-I, other samples also gave heat bursts as shown in Table III. It seems that the largest heat bursts occur for thick samples. This conclusion is consistent with the results of heat-after-death experiments [8,9] and with an experiment in which an explosion occurred [10].

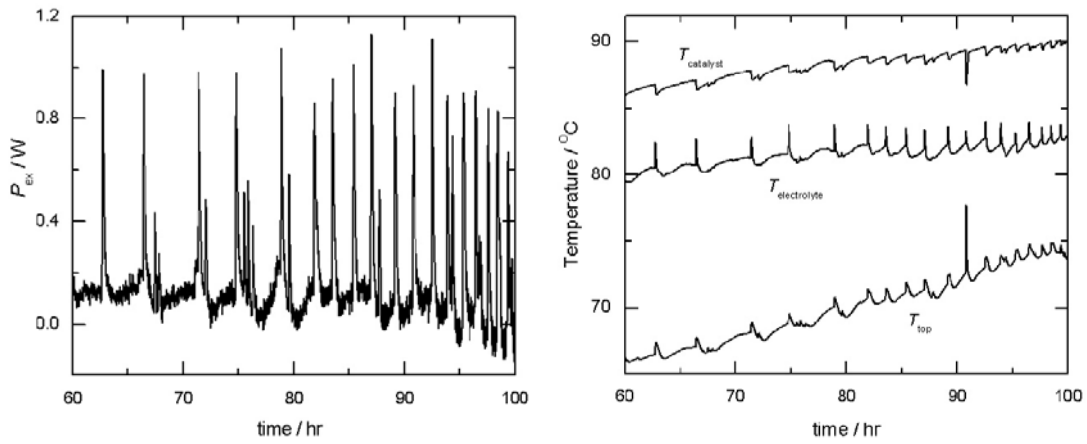

Fig. 2. Heat bursts and corresponding temperatures during electrolysis of sample Pd-I, a Pd tube, in Exp. No. 060620.

Table V. Dependence of excess power on run number.

Pd No	Run 1			Run 2[1]			Notes
	Exp. No.	P_{ex}/mW	Δm /mg h^{-1}	Exp. No.	P_{ex}/mW	Δm /mg h^{-1}	
A	050101	33 ± 13	269	050103	198 ± 16	15	See note 2
C	060209	0	253	060211	108 ± 29	48	See note 3
E	051127	0	207	051129	215 ± 56	231	See note 4
F1	051012	371 ± 60	384	051015	461 ± 20	200	See note 5
F2	051021	247 ± 87	200	051024	386 ± 38	225	See note 6
H	060404	50 ± 7	58	060406	129 ± 14	47	See note 7
H	060412	81 ± 21	32	060413	119 ± 11	62	See note 8

Notes: [1] Experimental conditions of Run 2 are same as those of Run 1.

[2] Dormant for 30 days before 050101.

[3] Reverse current for 1 hour before electrolysis in 060209.

[4] Dormant for 50 days before 051127.

[5] New sample.

[6] Reverse current for 1 hour before electrolysis in 051021.

[7] Reverse current for 1 hour before electrolysis in 060404.

[8] Reverse current for 1 hour before electrolysis in 060412.

A question of the excess heat in Pd|H_2SO_4+D_2O is the role of protium ions. In order to study this, we prepared heavy water electrolyte containing D_2SO_4 instead of H_2SO_4. The D_2SO_4 is 99.5+ at.% pure (Aldrich Chemical Company). The ratio by volume of D_2O:D_2SO_4 is 6.6:1, which is close to that of H_2SO_4 in D_2O (volume ratio of D_2O:H_2SO_4 is 6.7:1). Six runs with samples Pd-D and Pd-E from Dec. 12, 2005 to Jan. 4, 2006 gave maximum excess power of 115 ± 20 mW for Pd-D and 124 ± 54 mW for Pd-E, which are not greater than those obtained with D_2O + H_2SO_4 electrolyte. These results indicate the protium ion does not reduce the excess heat production. Currently, we use 99 at.% purity D_2O, not 99.9 at.% purityD_2O which we used previously; there has been no detectable difference in excess heat production.

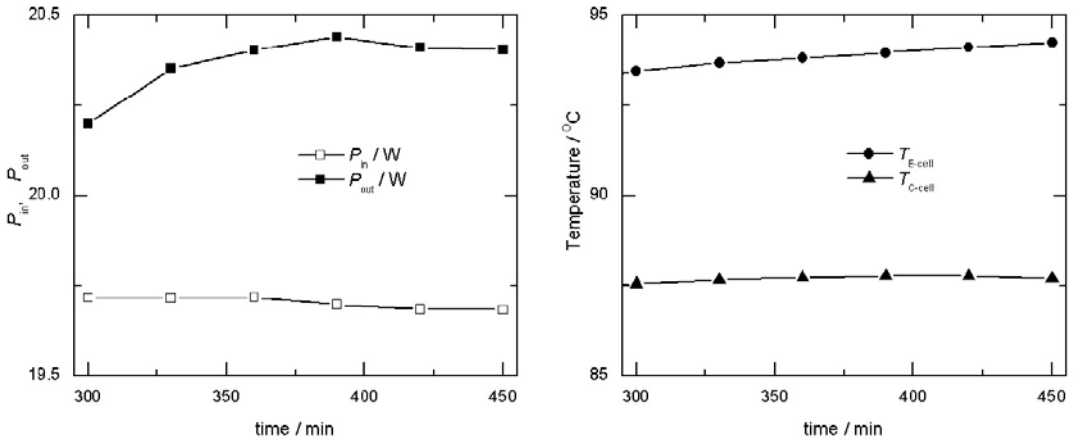

Fig. 3. Comparison between SEC and isoperibolic calorimetry (Exp. No. 050928). The graph on the left gives results obtained with the SEC. The average excess power is 759 ± 33 mW (without including mass loss) to 1,481 ± 35 mW (including mass losses of D_2O and H_2O, 0.62 and 1.09 g, respectively). The right graph shows average temperatures from eight thermocouples attached on the outside of both the Pd|D_2O and the Pt|H_2O cells. The input power of both cells is 9.60 ± 0.03 W, the applied current is 3 A for 7 hours and 30 minutes, the air temperature in SEC is 37 °C and the excess power of the E-cell is 783^{+716}_{-339} mW. The error of isoperibolic calorimetry mainly comes from the uncertainty of the proportion of D_2 (H_2), O_2, and D_2O (H_2O) vapor which escape due to poor recombination by the catalyst and a flexible seal between the cell body and its top. Increased pressure in the cell increases the rate of escape of gases from the cell. The rate of mass loss from a cell, shown in the data tables above, is a measure of the rate of escape of the gases.

In our experiments with H_2SO_4, the electrolyte was used for multiple runs. Only heavy water (about 20 grams needed after 3 A × 8 hrs electrolysis) was added to the old electrolyte to restore it to the original volume. Because of this, the H^+ concentration decreases with time in every run and from run to run. This means that our cell is a deuterium self-concentrated system and the isotopic purity of D_2O has negligible effect on excess heat production.

Another question is the validity of excess power measured by isoperibolic calorimetry which we reported previously [1–3]. Here we report the results of isoperibolic calorimetry and SEC obtained with the same electrolytic system. As described before [1–3], we used two cells with the same dimensions, one containing Pd|D_2O+H_2SO_4 and another containing Pt|H_2O+H_2SO_4. The concentration of H_2SO_4 in each cell is adjusted to ensure that the voltages and hence the input powers of these two cells are close to each other at the same current. These two cells are placed in a cardboard box (14 × 17 × 17.5 cm^3, 4 mm wall thickness) inside the SEC. Temperatures, current, voltages and the SEC signal are recorded with a data acquisition system. The results are shown in Fig. 3. We find that these two methods give the same excess power, within the precision of the measurements. This suggests that excess power results reported before [1–3] are likely to be accurate.

III. Scanning electron microscope and energy dispersive spectrometer characterization

III. 1. Silver

Before and after electrolysis, we characterized the surface morphology and elemental composition of Pd cathodes by scanning electron microscopy (SEM) and energy dispersive spectrometry (EDS). Most of samples show anomalous new element production [1–4]. We will report results of one sample, Pd-H, whose parameters are shown in Table IV. The photo of sample Pd-H after electrolysis for 186 hours is shown in Fig. 4, the electrode bends towards the anode during long time electrolysis as observed previously [4]. The fractures on the right edge of the convex side in Fig. 4(a) (or left edge of concave side in Fig. 4(b)) were formed during cold rolling, before electrolysis. The numbered white labels are areas studied by SEM and EDS.

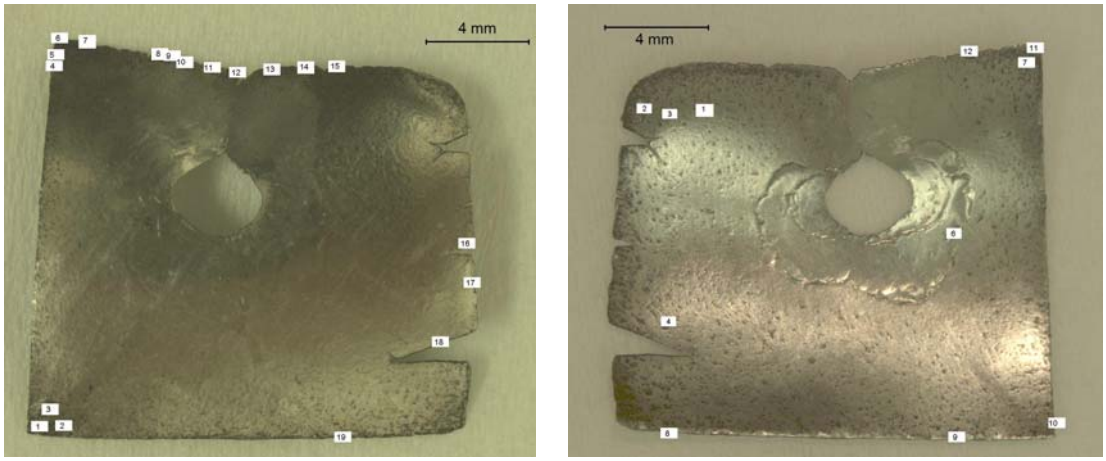

Fig. 4. Photos of Pd cathode H after electrolysis for 186 hours. (a) (left) The convex side, which faced away from the anode; (b) (right) the concave side, which faced the anode. The hole is used to connect the cathode lead wire as described in Ref. [4]. The white rectangles indicate the positions from which X-ray spectra were taken.

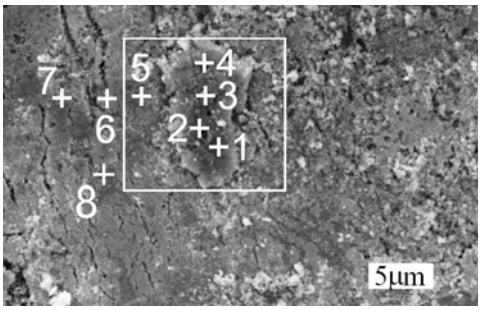

Fig. 5. SEM picture of region #16 in Fig. 4(a). SEM No. WS060505Pd-H-CV-i16-2kX.

Table VI. Relative atomic percent concentrations of silver at spots in Fig. 5.

Spot #	area*	1	2	3	4
Ag/(Pd+Ag)	55.3 ± 0.5	98.1 ±1.9	92.8 ± 0.2	96.5 ± 0.2	80.9 ± 0.3
Spot #	5	6	7	8	
Ag/(Pd+Ag)	6.0 ± 1.0	4.3 ± 1.5	3.4 ± 1.0	0	

* area = the square area with white case in Fig. 5.

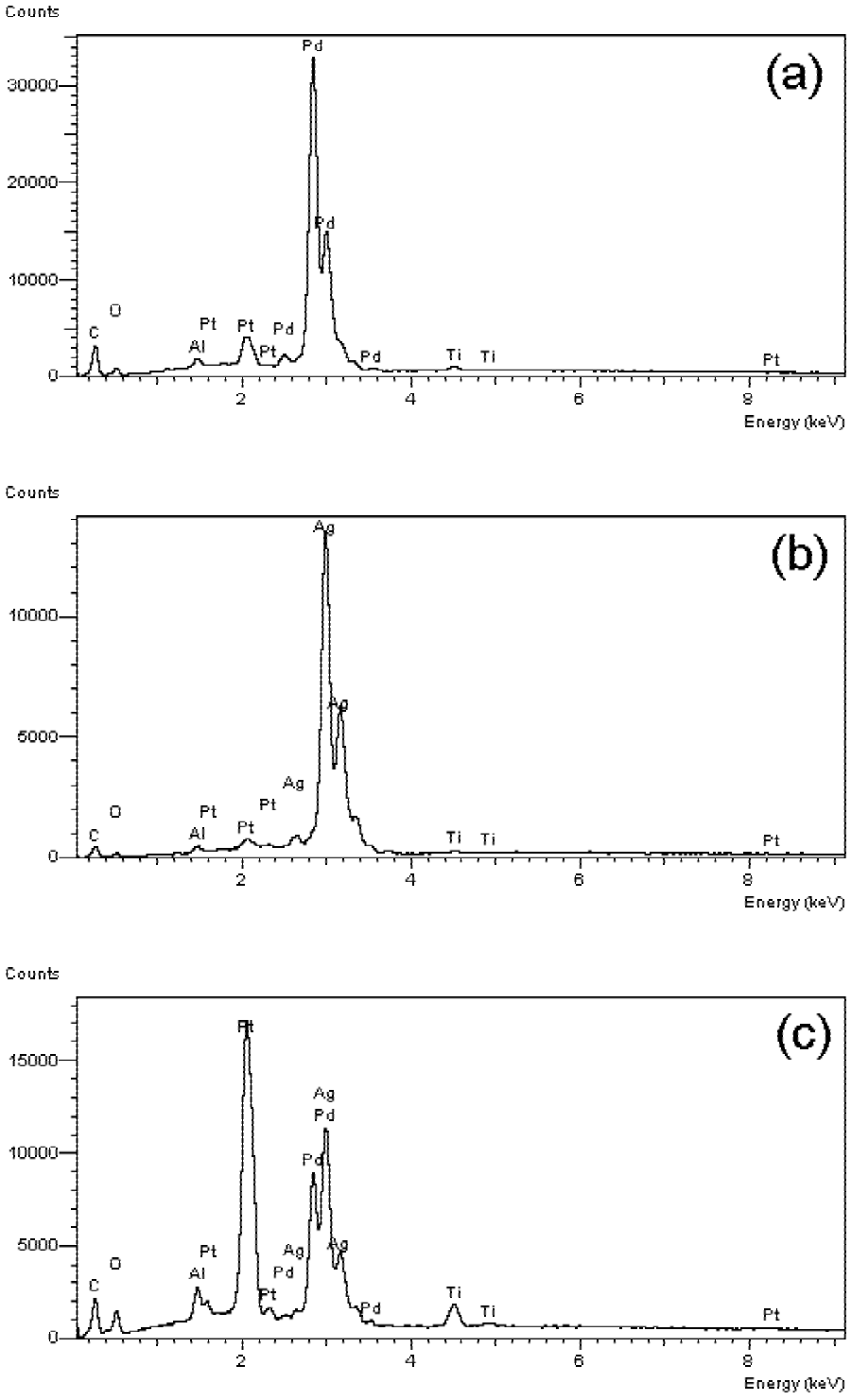

Fig. 6. Characteristic X-ray spectra of spot #8 (a), spot #1 (b) and square area (c) shown in Fig. 5.

Fig. 5 shows an SEM picture of region #16 in Fig. 4(a). Three characteristic X-ray spectra from this region are shown in Fig. 6. Fig 6(a) is from spot #8 in Fig. 5. The most prominent peaks in the spectrum are from Pd, the bulk metal. Other elements are from the electrolytic system: Pt is from the anode, which is slowly dissolved and deposited on the cathode; C most likely comes from back-streaming of hydrocarbons from the diffusion pump oil; Al and O are from the alumina recombination catalyst; and Ti is from the electrolyte. Ti was dissolved in the electrolyte before the experiments [3–5].

Fig. 6(b) is from spot #1, the most prominent element here is silver; other elements are the same as those in Fig. 6(a), except for the absence of Pd. Besides spot #1, other spots in the central black region of the foot-shaped feature in Fig. 5 are almost pure silver. We obtained the EDS spectrum in Fig. 6(c) from the central region in Fig. 5. Because the characteristic Lα X-ray of Ag is at 2.98 keV, it overlaps with Pd Lβ at 2.99 keV. The expected intensity ratio of Pd Lβ/Pd Lα is 0.42, whereas the ratio of these two peaks in Fig. 6(c) exceeds 1.0. As in our previous reports [2–5], we attribute the increase in this ratio to the presence of silver. The results of analysis of the EDS spectra are summarized in Table VI. The silver concentration is presented as a relative quantity for the convenience of comparison. Localized concentrations of silver were also detected along cracks in the microstructure shown in Fig. 5. Because of their irregular nature, these cracks probably formed during electrolysis rather than during cold rolling. These cracks also have localized concentrations of silver.

Another example is shown in Fig. 7 and Table VII.

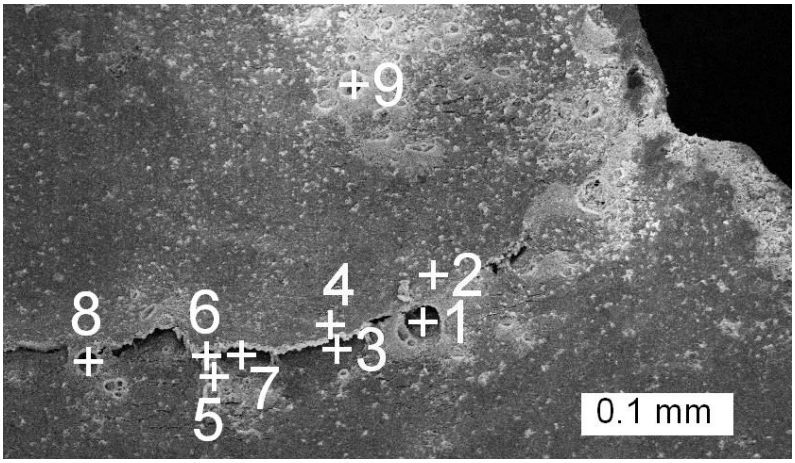

Fig. 7, SEM picture of region # 12 in Fig. 4(a). SEM No. WS060504Pd-H-CV-i12-150X.

Table VII. Relative atomic percent concentrations of silver at spots in Fig. 7. The other 5 spots which were tested have no silver.

Spot #	1	3	5	6	7
Ag/(Pd+Ag)	15.1 ± 2.6	9.4 ± 2.9	16.4 ± 6.0	11.6 ± 1.9	9.8 ± 2.2

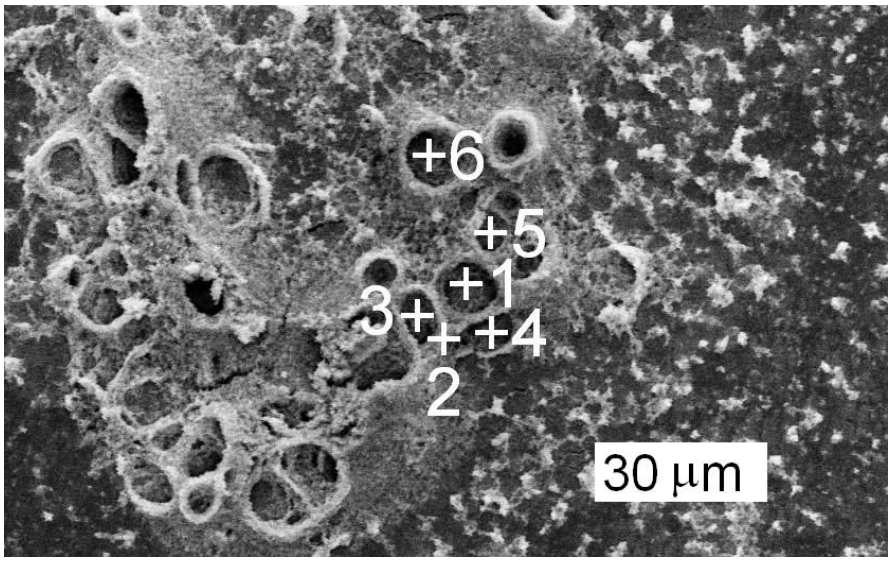

Fig. 8. SEM picture of region # 3 in Fig. 4(a). SEM No. WS060501Pd-H-CV-i3-500X.

Table VIII. Relative atomic percent concentrations of silver at spots shown in Fig. 8 under different acceleration voltages and at different times in 2006.

Time	Voltage/kV	spot 1	spot 4	spot 6
Apr 28 16:00-17:15	20	18.5 ± 3.7	9.2 ± 2.5	9.0 ± 3.9
Apr 28 17:45-18:15	20	18.1 ± 2.7	7.4 ± 1.7	15.0 ± 3.5
Apr 28 17:50-18:05	30	16.6 ± 2.5	8.3 ± 1.3	10.0 ± 1.8
May 1 10:20-10:45	20	15.2 ± 2.8	6.7 ± 1.4	12.4 ± 3.0
May 1 10:50-11:15	30	17.0 ± 2.3	8.2 ± 1.2	9.8 ± 1.7

The most common finding is that silver occurs in craters, such as those shown in Fig. 8. These craters with rims almost certainly formed during electrolysis. Pt deposition was concentrated on these protruding rims. We measured the silver concentration with different

accelerating voltages and at different times. The results in Table VIII show that there are no obvious changes in silver concentration due to either the increase in accelerating voltage or to the passage of time.

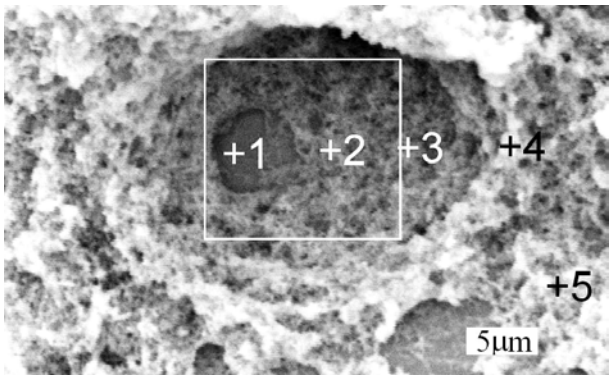

Fig. 9. SEM picture of crater at another time. SEM No. WS060607Pd-H-CC-i2-2kX.

Table IX. Relative atomic percent concentrations of silver in areas and spots shown in Fig. 9.

Spot #	wa*	area**	1	2	3	4	5
Ag/(Pd+Ag)	1.2 ± 0.5	5.6 ± 0.4	6.8 ± 0.4	5.6 ± 0.3	6.3 ± 0.4	3.6 ± 0.6	1.2 ± 0.5

* wa = whole area in Fig. 9.

** area = the square area with white case in Fig. 9.

We have studied the crater shown in Fig. 9 in detail as listed in Table IX. This crater is also located on an edge on the concave side of the same sample. From these results it is concluded that the silver concentration varies by about a factor of 5 from the lowest in spot 5 to the highest in spot 1.

The silver concentration in all 19 regions in Fig. 4(a) is summarized in Table X. Concentrations labeled P were obtained with the electron beam fixed in one spot on the cathode, and A designates concentrations obtained with the electron beam scanning a known area of the cathode. The silver production on the concave side in Fig. 4(b) is summarized in Table XI.

Table X. Summary of relative Ag concentration at regions on the convex side of the Pd cathode (facing away from the anode) shown in Fig. 4(a).

Region #	1	2	3	4	5	6	7	8	9	10
Maximum Ag/Pd	0	7.7	18.5	99.1	97.9	80.4	0	11.1	9.2	8.4
Mode		P	P	A	A	P		P	P	P
Region #	11	12	13	14	15	16	17	18	19	
Maximum Ag/Pd	7.0	16.4	5.1	7.2	40.3	98.1	31.7	68.4	26.6	
Mode	P	P	P	P	P	A	P	P	A	

Table XI. Summary of relative Ag concentration at regions on the concave side of the Pd cathode (facing the anode) shown in Fig. 4(b).

Region #	1	2	3	4	6	7	8	9	10	11	12
Maximum Ag/Pd	0	5.7	0	0	5.1	5.2	8.4	17.1	12.1	13.2	95.8
Mode		P			P	P	P	P	P	A	A

Besides the H sample Pd cathode, silver was also detected on other samples, as reported before [4].

Some conclusions can be reached concerning the location of silver on the cathode after electrolysis: (1) Silver occurs preferentially around the sample edges rather than in the central area, as observed before [1–6]; (2) silver is found more frequently on the back (convex) side of the Pd cathode than on the side facing the anode (concave side). Of course, there is another possibility: the silver on the concave side was covered by a Pt deposition layer, which is thicker than that on the convex side.

III.2. Nickel

Another anomalous element is nickel, which was detected in regions # 2 and #3 in Fig. 4(b). The SEM picture, X-ray spectrum of spot #1, and EDS measurement results from region #2 are shown in Figs. 10 and 11, and Table XII, respectively, where Ni/(Pd+Ni+Ag) from different spots ranges from 0.9 to 2.1 at.%. The average value for the whole area is Ni/(Pd+Ni) = 1.3 at.%. Region #3 in Fig. 4(b) also contains nickel, Ni/(Pd+Ni) = 1.1 to 1.9 at.% , in various spots. The nickel is concentrated in the upper left corner on concave side of the Pd-H sample. For example, Ni is not present in any of the spectra in Fig. 6. We also have observed Ni, on the order of 1 at.% or less, in other samples.

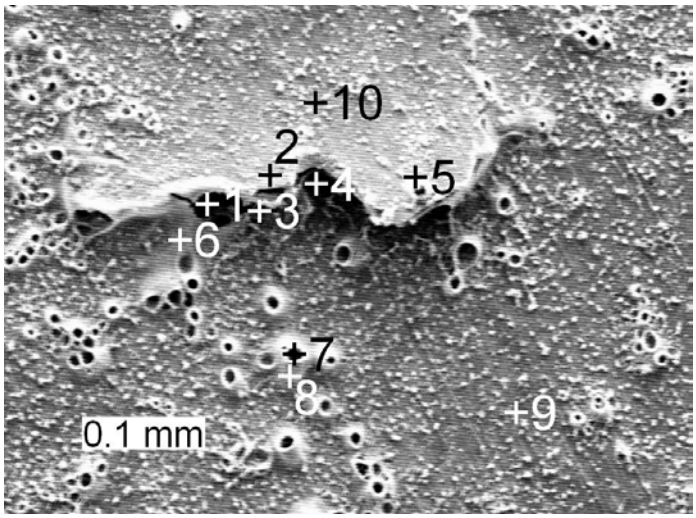

Fig. 10. SEM picture of region #2 in Fig. 4(b). SEM No. WS060424Pd-H-CC-i2-150X

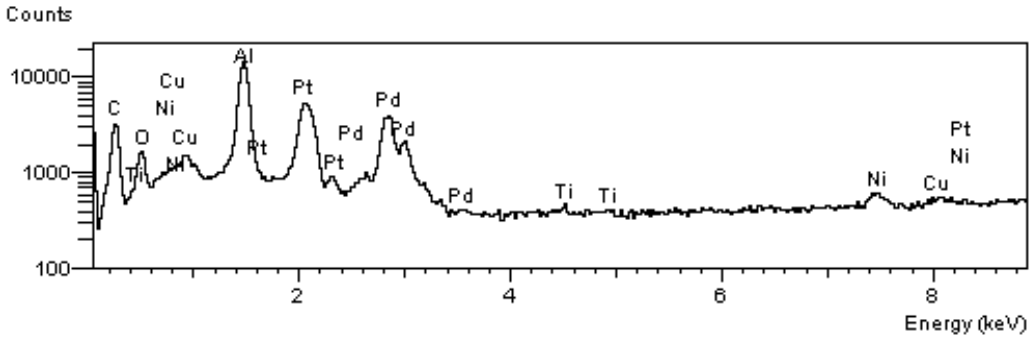

Fig. 11. Characteristic X-ray spectrum of spot #1 in Fig. 10. EDS No. WS060424Pd-H-CC-i2-150X-s1.

Table XII. Summary of relative Ag and Ni atomic percent concentration at regions shown in Fig. 10.

Spot #	Ag/(Pd+Ni+Ag)	Ni/(Pd+Ni+Ag)
wa*	0	1.3 ± 0.2
1	0	2.1 ± 0.1
2	5.7 ± 1.9	2.1 ± 0.2
3	0	1.1 ± 0.1
4	0	1.3 ± 0.1
5	0	1.5 ± 0.1
6	0	0.9 ± 0.1
7	3.3 ± 1.1	1.7 ± 0.1
8	0	1.2 ± 0.1
9	0	1.4 ± 0.1
10	0	1.9 ± 0.1

* wa = whole area in Fig. 10

What is the origin of this nickel? Ni was listed as “not detected” in the chemical analysis provided by the vendor of the Pd foil. It is very unlikely to have resulted from the cold rolling process or from electrodeposition because it is highly localized near one corner of the cathode. If it is the result of either contamination from the rolling mill or from electroplating it should not be highly localized on only one corner of the cathode. It could not have resulted from SEM systems because the stainless steel components of the SEM chamber also contain Fe and Cr. Fe and/or Cr are not present in any of the spectra. The SEM does not have components made of pure Ni. Therefore, the origin of the Ni is not known.

IV. Discussion

Since the discovery of excess heat in 1989 [11], the reproducibility has been a difficult problem [7]. Our results suggest a reason why Fleischmann and Pons and other groups observed excess heat using Dewar-type electrolytic cells and isoperibolic calorimetry [8,11–13], but some groups using mass-flow calorimetry, had difficulty detecting excess heat,

or the reproducibility was very poor. The reason is that the latter method involves a low temperature, semi-isothermal measurement. The temperature difference between the electrolytic cell and the water flowing during electrolysis is very small. Therefore, this system has to be stimulated by various methods, e.g., high input power, laser irradiation etc. [7] Even then, the reproducibility is still low because the cell temperature is not high enough.

Our experiments using small diameter Pd tubes as cathodes produced many more heat bursts than flat Pd foil cathodes. Further study using Pd tube cathodes is warranted.

Using an EDS attached to a SEM; we again have found localized concentrations of silver on the surfaces of Pd cathodes after electrolysis. On a few of the cathodes, we also found localized concentrations of nickel. Further study, such as the determination of isotopic ratios before and after electrolysis, is needed to aid in understanding the origin of the Ag and Ni.

Acknowledgement

This research was supported by a grant from the New York Community Trust.

References

1. Ambadkar A. and Dash J., Electrolysis of D_2O with a palladium cathode compared with electrolysis of H_2O with a platinum electrode: procedure and experimental details, see: http://www.newenergytimes.com/Library/2003DashJ-ColdFusionRecipe.pdf
2. Dash J. and Ambadkar A., Proc. ICCF11, Marseille, France, Oct 31 to Nov 5, 2004, P. 477.
3. Wang Q. and Dash J., Proc. ICCF12, Yokohama, Japan, Nov 27 to Dec 5, 2005, P. 140.
4. Zhang W.-S. Dash J. and Wang Q., Proc. ICCF12, Yokohama, Japan, Nov 27 to Dec 5, 2005, P. 86.
5. Dash J., Noble G. and Diman D., Trans. Fusion Tech., 1994, V.26, No.4T, P.299.
6. Miguet S. and Dash J., J. New Energy, 1996, V.1, P.23.
7. Storms E., Infinite Energy, 1998, V.4, No.21, P.16.
8. Pons S. and Fleischmann M., Trans. Fusion. Tech., 1994, V.26, No.4T, P.87.
9. Rothwell J., Cold Fusion and the Future, 2004, lenr-canr.org. P.13.

10. Zhang X.-W., Zhang W.-S. and Wang D.-L. *et al*., Proc. ICCF3, Nagoya, Japan, Oct 21 to 25, 1992, P.381.
11. Fleischmann M., Pons S. and Hawkins M., J. Electroanal. Chem., 1989, V.261, P.301; errata 1989, V.263, P.187.
12. Szpak S., Mosier-Boss P.A., Miles M.H. and Fleischmann M., Thermochim. Acta, 2004, V.410, P.101.
13. Miles M. Proc. ICCF10, Cambridge, MI, USA, Aug 24 to 29, 2003, P.23.